Corrosion effects on the mechanical properties of reinforcing steel bars. Fatigue and σ-ε behaviour.

Ignasi Fernandez*[1], Jesús Miguel Bairán[1], Antonio R. Marí[1]

[1] Department of Construction Engineering, Polytechnic University of Catalonia, Jordi Girona, 1-3, Barcelona 08034, Spain.

*corresponding author: ignasi.fernandez-perez@upc.edu

Highlights:

- Experimental studies on fatigue and monotonic tests with corroded an uncorroded steel bars.
- Variation of the mechanical properties of corroded reinforcement as a function of the corrosion degree
- Pit characterization in the critical cross-section.
- Influence of the corrosion degree on the fatigue life.

Abstract: Corrosion of steel reinforcement is one of the most severe problems of durability in reinforced concrete structures. A good understanding of the corrosion effects on the reinforcing steel mechanical properties is necessary to adequately assess impaired structures. A study of the mechanical response of corroded reinforcement subjected to monotonic and cyclic loads by means of an experimental study is presented in this work. More than 180 corroded specimens, 40 monotonic and 140 fatigue tests were performed. Relationships between corrosion penetration and the mechanical properties of reinforcing steel bars were identified. In addition, a study of the

influence of the pit geometry on the fatigue life was carried out. A severe non-linear reduction in the mechanical properties studied, related to the corrosion degree was observed. These phenomena can provide relevant information for the assessment of existing structures and for life cycle evaluation.

Keywords: Corrosion, Tensile properties, Mechanical properties, Fatigue, Durability

1. Introduction

Corrosion of the reinforcement steel bars is one of today's most frequent and significant types of damage in existing reinforced concrete structures. Therefore, the study of the structural effects of bars corrosion is crucial for determining the structural performance and residual strength of impaired structures. Volumetric expansion of corrosion products may induce splitting stresses along corroded reinforcement, and damage to the surrounding material. Generally, the splitting stresses are not well tolerated by concrete, resulting in cracking and eventually spalling of the concrete cover. As the reinforcement becomes more exposed, the corrosion rate may increase and facilitate the deterioration process. Either generalised corrosion, which affected uniformly to the whole bar length, or pitting corrosion, which affected in a specific part of the bar, have important effects on the mechanical behaviour of the steel reinforcement bars. In this work are presented artificially corroded specimens by means of induced current methods, in which corrosion degree is defined as the loss of mass due to corrosion with respect to the uncorroded bar, that could be described as the corrosion penetration expressed in % of cross-section reduction. It is obtained by means of gravimetric methods following the ASTM code [19]. The specimens were cleaned by means of mechanical methods.

One significant steel corrosion effect is the change in the mechanical properties of reinforcing bars. Even though most of the investigations are not focused on this effect, steel reinforcement corrosion yields into material mechanical properties changes [1–4]. The study of the local impacts of corrosion is critical to define the mechanical properties of corroded steel bars to be used in structural models, in order to adequately assess the structural behaviour and safety at local or global levels. The change in steel behaviour may give place to an unexpected structural response, producing even undesired brittle failures.

53 The classical approach to consider corrosion of steel reinforcement in the response of concrete
54 structures has been to consider a reduction of nominal cross-section area proportional to the
55 corrosion degree. However, both generalized and pitting corrosion produce other effects than just
56 the loss of steel area, such as stress concentration at the notch tip. In addition, the displacement of
57 the centre of gravity of the cross-section due to a non-uniform corrosion or because of the pit
58 itself produces a non-uniform stress distribution along the pitted cross-section. Furthermore,
59 some modern production systems of reinforcing bars, such as TEMPCORE®, produces
60 heterogeneous material properties throughout the steel cross-section, being the apparent σ-ε
61 characterization of the bar, the mean response of the heterogeneous section. Specifically annular
62 distribution of the mechanical properties takes place for this steel manufacture system [5–9].
63 Obviously the loss of part of the cross-section modifies the balance of the mechanical properties
64 distribution not only because of the reduction of steel cross-section itself but because of the loss
65 of the external crowns of material which provides higher load capacity to the outfit.

66 Several experimental studies were performed during the last years to evaluate the influence of the
67 corrosion degree of steel bars embedded in concrete on their mechanical properties [1–4,10–15].
68 A smaller number of studies have been undertaken on the evaluation of the response of corroded
69 steel bars subjected to low-cycle loads [16–18]. Even fewer investigations are found in the
70 literature studying the corroded steel behaviour under high-cycle loads [15].

71 In this research work, a study of the mechanical reinforcing steel properties, either corroded or
72 uncorroded, using monotonic tensile tests and cyclic loading fatigue tests, is presented. Two
73 experimental phases were carried out in order to define the main mechanical properties of 10mm
74 and 12 mm diameter artificially corroded steel bar. Phase 1 consisted on monotonic tests while
75 phase 2 encompassed high-cycle load tests. The variation of the mechanical properties is related

76 to the corrosion degree by comparing the results with those obtained from tests performed on
77 uncorroded bars

78 Along the monotonic tests performed in experimental phase 1, the main parameters defining the
79 σ-ε curves of corroded steel were measured. A total of 40 specimens of 310 mm to 320 mm
80 lengths were satisfactorily tested having corrosion degrees ranging from 8% to 22%.

81 At Phase 2, 140 specimens of 310 to 320 mm length with corrosion degrees ranging from 8% to
82 28% were tested under several cyclic loads. Three different stress ranges (ΔS= 150 MPa, 200
83 MPa and 300 MPa) were defined in order to evaluate the influence of the stress range on the
84 fatigue life of corroded bars. These stress ranges were selected to represent the stress levels that
85 take place in reinforcing bars under common service load conditions. By applying those load
86 levels, it is possible to measure the fatigue life reduction at the service load level with respect to
87 the uncorroded steel. The characteristic pit was measured on all the tested specimens in order to
88 evaluate its influence on the reduction of fatigue life.

89 **2. Materials**

90 B500SD (see Table 1 for different EU denominations and standards) reinforcing steel was used in
91 the monotonic and fatigue test for corroded and uncorroded specimens. Uncorroded steel main
92 properties are described in Table 2. Figure 1 shows the measured σ-ε behaviour for the two steel
93 diameters used in this work.

3. Corroded steel bars under cyclic and monotonic loads

3.1 Test setup and execution

The tests presented next are part of a larger experimental campaign , conducted at the Universitat Politècnica de Catalunya – Barcelona Tech (UPC), which encompassed tests of statically indeterminate beams under different corrosion degrees to assess the structural effects due to steel reinforcement corrosion, Figure 2. This work focuses on direct monotonic and cyclic loading tests of the corroded steel reinforcement extracted from the above mentioned beams having the underlying purpose of extending the existing database of monotonic test of corroded steel bars and contributing to a new significant database of corroded specimens tested under cyclic loads.

Steel bars were extracted from beams exposed to different corrosion degrees by means of induced corrosion procedure [20–22]. The beams were casted incorporating in the mixture 4% NaCl in cement weight, breaking the steel passive protective layer. The applied current density was designed to assure the desired corrosion degree in each case. This was done through a DC power supply with an ammeter to monitor and fix the current intensity. The current direction was defined fixing the reinforcing steel as anode and the stainless steel bar as the cathode. A schematic representation of the accelerated corrosion test setup is presented in figure 3a. Each beam had two different bar diameters (10 mm and 12 mm). Monotonic load tests were carried out in the continuous beams and subsequently bars were carefully extracted from the non-critical section of the beams in order to perform the characterization of the corroded bars under monotonic and cyclic loads.

Using gravimetric methods, the loss in weight of the specimens was determined according the ASTM code [19]. A pressure sand cleaning method was applied in order to remove both rust and

bonded cement, Figure 3b. In total 241 specimens were obtained covering corrosion degrees from 7% to 28% for both the 10 mm and the 12 mm diameter bars, see Figure 4.

3.2. Monotonic test

The tests were carried out following the standard recommendations [23] and an INSTRON 8803 Universal Testing machine.

The specimens employed for monotonic testing had between 310 mm and 320 mm length. The ends of the tested specimens were affixed by two clamps, which were used to transfer directly the load to the specimen. The tested free length for all the specimens was 170 mm letting 70/75 mm length for each clamp. Monotonic tests were conducted by means of displacement control. The load was applied directly to the bar controlled by the load cell placed on the top of the hydraulic jack. Total displacement, as well as deformation, were registered too. Specimen deformation was measured using a displacement transducer of 50 mm length positioned in the middle of the tested bar (see Figure 5). The load was applied until specimen failure. Uncorroded specimens were also tested to compare and assess the influence of the corrosion degree on the mechanical properties. In total, 40 specimens were tested satisfactorily. The weakest section, where most likely the bar would fail, was identified for all the specimens by means of the description of the observed critical pit. The critical pit geometrical specs, pit depth and pit length, were measured using a Vernier calliper (Figure 9). Recent studies tried to relate the pit characteristics with the steel bar corrosion degree in bars submitted to accelerated corrosion methods [24].

3.3 Fatigue test

Fatigue specimens were between 310 mm and 320 mm large. The test setup was similar to the monotonic tensile test. However, cyclic load test was conducted by means of load control. The load was applied directly to the bars controlled by the load cell placed on the top of the hydraulic

jack. Total displacement, as well as deformation, were registered too. Specimen deformation was measured using a displacement transducer of 30 mm length positioned in the middle of the specimen. Each measurement was stored every half second by means of a data logger, see Figure 6. Also, the characterization of the most probably failure cross-section was done by means of the definition of the critical pit geometry using a Vernier calliper (Figure 9).

Three different cyclic loads were defined characterized by the following stress ranges: 150 MPa, 200 MPa and 300 MPa ($\Delta S = S_{max} - S_{min}$), considered as typical stresses due to the service loads. The stress range was defined based on the uncorroded section steel. A non-zero minimum stress was used to avoid compression in the bar and its possible buckling effects. The maximum stress (S_{max}) was, for uncorroded specimens, lower than $0.6*f_{y,}$ which is the theoretical threshold below what there is no fatigue life reduction. Considering the nominal diameter of uncorroded specimens and the stress range chosen, the maximum and minimum applied loads were defined. The applied load range for corroded specimens was the same as for uncorroded specimens, taking into account the uncorroded nominal diameter, see eq 1.

$$(1)\quad \Delta S = S_{max} - S_{min} = \frac{F_{max}}{A_0} - \frac{F_{min}}{A_0}$$

Using these load ranges, it was possible to directly compare the effect of the different corrosion degrees in a corroded structure with the same design load with respect to the uncorroded one. The applied loads considering the three mentioned stress ranges are described in Table 3. No specimens of 10 mm diameter were tested with ΔS= 150 MPa. The load was applied following the same wave shape cycles of 15 Hz frequency (see Figure 7). In the same figure, the main variables for the fatigue problem are stated, S_{max}, S_{min}, S_m, S_a and ΔS. The specimens were tested at room temperature.

A total of 140 specimens were tested with corrosion degrees between 8% and 28%. Some specimens were discarded due to an induced failure in the clamps zones because of stress localization effects, see Table 4.

4. Test results

Used nomenclature for the test description was XX-YY-ZZ, where XX corresponds to the type of test performed (MT for monotonic or FT for fatigue test), YY is 10 or 12 and corresponds to the specimen diameter and YY the test number.

4.1 Effect of corrosion on the reinforcing steel mechanical properties

Appendix A. Table 1, shows the detailed results of the monotonic tested members. In the table the nominal diameter of tested bars, the yielding load in kN, the ultimate load in kN (maximum resisted load by the specimen), the strain corresponding to the maximum load, ε_{max}, the registered strain on failure, ε_u, and the modulus of elasticity, E, in N/mm^2 for each specimen, are presented. In addition, for easier comparison between corroded and uncorroded specimens, the apparent yielding stress f_y^* (elastic limit stress in MPa) and the apparent strength f_{max}^* (maximum resisted stress in MPa). The apparent strength is defined as the stress obtained dividing the maximum load by the thetheoretical area that the bar would have, considering a generalised corrosion for the given corrosion degree (see Figure 8b).

(2) $$g = 1 - \frac{A_c}{A_0}; \qquad f = \frac{1}{1-g}$$

Where A_c is the reinforcing steel area under generalized corrosion and A_o is the nominal area.

The characterization of the critical pit observed in each specimen is described by means of the pit depth (p) and the pit length (l) (Figure 9). Figure 10a depicts typical σ-ε curves for 10 mm and 12

182 mm diameter bars with various corrosion degrees (8-10%). This figure shows a high scatter in
183 measured strains in all tests, even considering them had same corrosion degree. Figure 10b
184 compares the strains measured with the test machine and that measured with the extensometer,
185 which had a 50 mm base measurement. It can be seen that in uncorroded specimens, higher
186 strains were registered by the machine than by the extensometer, as it was expected (since they
187 include machine deformations, slip in the clamps, etc..). Instead, corroded members showed the
188 opposite behaviour, indicating the strong influence of local effects on the pit during the tensile
189 test, which produce higher strains in the critical pit zone and surroundings.

190 *4.1.1 Yielding and ultimate load capacity*

191 Figure 11 describes the evolution of some parameters presented in Appendix A. Table 1 with
192 respect to the measured corrosion degree. As expected, there was a significant drop of all of the
193 parameters studied with respect to that of uncorroded steel bars due to different causes. Yielding
194 stress and maximum stress presented a decreasing tendency with respect to the corrosion degree,
195 which may be fitted by means of a polynomic function with a coefficient of correlation between
196 0.647 and 0.749 for 12 mm diameter. The correlation coefficient for 10 mm diameter specimens
197 was from 0.54 to 0.61 most, probably because there were much less tested specimens, especially
198 for high corrosion degrees.

199 Previous studies [1,3,11] already reported a decreasing behaviour of the elastic and ultimate
200 stresses of corroded bars, however, in those studies a linear relationship with the corrosion degree
201 was stated. Those works also noticed that the reduction of the tensile properties slightly decrease
202 respect to those of uncorroded specimens. In this work, the tensile stresses were obtained
203 dividing the registered load with respect to an equivalent corroded cross-section area of the bar,
204 which represented the generalised corrosion degree measured. Using that value allows

205 establishing a trustworthy relationship between corrosion degree and reduction of cross-section.
206 So it is considered that the corrosion degree is a global variable of the specimen (corrosion
207 penetration or generalised corrosion), not the particular corrosion degree of the critical cross-
208 section (which presented a higher loss of mas due to the critical pit). Using the generalised
209 corroded cross-section area hypothesis, the effective stress or modulus value decreased with
210 respect to that of the value obtained using the real cross-section diameter. See Figure 8a, obtained
211 by means of a 3D scan technique, by which the aforementioned hypothesis is described.

212 Also in Figure 11 is it possible to observe the theoretical expected values both ultimate and
213 yielding stresses. Those values were obtined by the queficient Fy_0 or Fu_0 (uncorroded specimen
214 values) with respect to the equivalent area associated to each corrosion degree, which correspond
215 to the classical approach to consider the corrosion in reinforced concrete structures. As it is
216 described, the effect of corrosion produces a non-linear behaviour, which is in addition more
217 harmful than expected.

218 *4.1.2 Modulus of elasticity and ductility*

219 The elastic modulus and the measured strains at maximum load (ε_{max}) showed higher scatter than
220 fy* and fu*, see Figure 12. It was very difficult to establish a good correlation between these
221 values and the corrosion degree. However, the measured values also decreased with the corrosion
222 degree. In any case the correlation coefficient for 12 mm diameter was always lower than 0.65
223 for the three parameters. Mechanical fracture theory could justify that registered dispersion. In
224 general, a reduction of ductility was observed for all the specimens, behaviour which was also
225 observed by other researchers [11,25]. Despite of the scatter data did not allow to establish any
226 trustworthy relationship with the corrosion degree.

227 *4.1.3 Discussion*

228 Figure 13 describes the variation of the maximum and the yielding loads with respect to those of
229 uncorroded steel for the different corrosion degrees measured. In both the 10 mm and the 12 mm
230 diameter bars, it is possible to observe a different growing rate between the corrosion degree and
231 the ratio of both parameters. The reduction of capacity decreased linearly with the corrosion
232 degree as it was expected. Also the theoretical values of expected loads are described, which
233 resulted higher that the experimental ones. Other phenomena, such as stress concentration in the
234 pit [10] and non-homogeneity of the steel bar cross-section (because of the production procedures
235 [6,8,17]) must be taken into consideration to justife this divergent behaviour. Both 10 mm
236 diameter and the 12 mm diameter described the same behaviour.

237 *4.2 Effect of corrosion on the fatigue behaviour*

238 The detailed results of the cyclic load tests in terms of total resisted cycles for the corroded
239 specimens extracted and characterised from the beams are shown in Appendix A. Table 2. The
240 characterization pit parameters such depth (p) and length (l) are also included, as well as the
241 stress range to which the bar was submitted (ΔS), corresponding to the applied load of Table 3.

242 *4.2.1 Influence of pit geometry*

243 Figure 14a describes the evolution of the pit depth with respect to the corrosion degree
244 measured. It is possible to observe a large scatter of the obtained results. However, a clear trend
245 of the values was depicted indicating the higher pit depth the higher corrosion degree was. The
246 dimensionless ratio pit depth divided bar diameter was used to compare within the different
247 tested diameters. That trend is described by the linear adjustment defined in figure 14a., even
248 though a poor correlation coefficient (0,45) is obtained. The same comparison is stated in figure
249 14b for the pit length. Also, the length value was divided by the nominal bar diameter to obtain a
250 dimensionless parameter and make easier the comparison between all the specimens. Again a

poor correlation between the corrosion degree and length/diameter value was observed. In any case, the pit length increment is lower with respect to the corrosion degree than for pit depth. In figure 14c a comparison between the pit depth and the pit length is presented, showing that the pit depth is a parameter more sensible to corrosion degree than pit length. In addition the effect of stress concentration has less influence than the loss of steel area, because that effect is more sensitive to the longitudinal pit angle (figuring out the pit geometry like an elypsse where the long diameter is the length and the other diameter is the depth).

Lastly, Figure 14d describes the overall behaviour of the corroded specimens depicting the total resisted cycles with respect to its corrosion degree. As it is shown in that figure, the number of cycles decreases quickly with the corrosion degree .

Figure 15a shows that the effect of the pit length on fatigue life, N, was practically constant for ratios length/diameter higher than two. For those, the effect on fatigue life can be considered less relevant in comparison with pit depth. However, as it is shown in figure 15b the fatigue life always decreased with the ratio p/ϕ (ratio between pit depth and nominal diameter).

4.2.2 Influence of stress range

As it is shown in Figures 16a and 16b, the fatigue life of corroded specimens is reduced significantly with respect to that of uncorroded steel. The reduction of fatigue life of corroded specimens could be adjusted quite accurately following a negative exponential adjustment. An attenuation rate is observed with the decrease in the stress level, as it is observed in both figures and mainly in Figure 16a for stress ranges of 300, 200 and 150 MPa. A similar behaviour was also documented by other authors [1,15] for naturally corroded specimens submitted to different stress ranges, however in this work it was noticed that all specimens showed the same behaviour despite the stress range applied.

The results obtained suggested that the corrosion of steel reinforcement has no significant effect on fatigue life for very low corrosion degrees, although for higher corrosion degrees a severe reduction of fatigue life was observed.

5. Conclusions

Based on the results of the study performed, the following conclusions can be drawn:

(1) Yield and ultimate stresses measured in the monotonic tests were found strongly dependent on the corrosion degree. Corrosion of steel highly reduces the yielding and ultimate stresses.

(2) Modulus of elasticity and measured strains present a higher dispersion than yield stresses and strength. In addition, a premature failure was observed resulting in a severe reduction in ductility.

(3) Using the hypothesis of uniformly corroded cross-section, based on the actual corrosion penetration, proved useful to describe the evolution of the mechanical properties. This approach is considered to yield more reliable results compared to using the real corroded failure cross-section. Additionally, it was found that experimental data of the tensile capacity of corroded bars underestimated the expected theoretical capacity calculated according to a mere reduction of the cross-sectional area.

(4) In all cases studied, the reduction of mechanical properties is not proportional to the corrosion degree. A strong influence of other parameters such as stress concentrations at the top of the pits, non-homogeneity of steel bar properties (due to TEMPCORE® production system) or the displacement of the center of gravity due to a non-uniform loss of mass was observed. The yield and ultimate stresses can be related to the corrosion

degree by means of a parabolic function when the stresses are referred to the idealized generalized corroded diameter.

(5) Pit depth has a higher influence on fatigue life behaviour than pit length. Pit length has no effect on fatigue life for length/diameter ratios higher than 2. Instead, the deeper the pit, the bigger is the impact of the ratio depth/diameter.

(6) Fatigue life for corroded bars is severely reduced with respect to that of uncorroded steel bars. For very little corrosion degrees, the effect is negligible. For high corrosion degrees a negative exponential may adequately describe the decreasing numer of resisted cycles. In addition, very high corrosion degrees present a severe reduction of fatigue life independent of the stress range applied.

Further studies on the effects of low corrosion degrees, from 0% to 8% would be desirable. In addition, to study naturally corroded specimens would be of interest to confirm the effect of pit characteristics on fatigue and tensile properties.

Acknowledgments

The authors wish to acknowledge the financial support of The Ministry of Economy and Competitiveness of the Government of Spain (MINECO) for providing funds for projects BIA2009-11764, as well as BIA2012-36848 and the European Funds for Regional Development (FEDER). The financial support of Infrastructures de Catalunya (ICAT) is also highly appreciated.

Appendix A

References

[1] Zhang W, Song X, Gu X, Li S. Tensile and fatigue behavior of corroded rebars. Constr Build Mater 2012;34:409–17. doi:10.1016/j.conbuildmat.2012.02.071.

[2] Apostolopoulos CA. Mechanical behavior of corroded reinforcing steel bars S500s tempcore under low cycle fatigue. Constr Build Mater 2007;21:1447–56. doi:10.1016/j.conbuildmat.2006.07.008.

[3] Apostolopoulos CA, Papadopoulos MP, Pantelakis SG. Tensile behavior of corroded reinforcing steel bars BSt 500s. Constr Build Mater 2006;20:782–9. doi:10.1016/j.conbuildmat.2005.01.065.

[4] Apostolopoulos CA a., Papadakis VGG. Consequences of steel corrosion on the ductility properties of reinforcement bar. Constr Build Mater 2008;22:2316–24. doi:10.1016/j.conbuildmat.2007.10.006.

[5] Çetinel H, Toparlı M, Özsoyeller L. A finite element based prediction of the microstructural evolution of steels subjected to the Tempcore process. Mech Mater 2000;32:339–47. doi:10.1016/S0167-6636(00)00009-0.

[6] Sankar I, Rao K, Gopalakrishna A. Optimization of steel bars subjected to Tempcore process using regression analysis and harmony search algorithm. J Sci Ind Res 2010;69:266–70.

[7] Nikolaou J, Papadimitriou G. Microstructures and mechanical properties after heating of reinforcing 500 MPa class weldable steels produced by various processes (Tempcore, microalloyed with vanadium and work-hardened). Constr Build Mater 2004;18:243–54. doi:10.1016/j.conbuildmat.2004.01.001.

[8] Simon P, Economopoulos M, Nilles P. Tempcore: a new process for the production of high quality reinforcing bars. Iron Steel Eng 198AD;61:55–67.

[9] Bairan JM, Marí a. R, Ortega H, Rosa JC. Efecto del enrollado y enderezado en las propiedades mecánicas de barras de acero de diámetro medio y grande fabricadas en rollo. Mater Construcción 2011;61:559–81. doi:10.3989/mc.2011.60110.

[10] Almusallam AA, Al-Gahtani AS, Aziz AR, Dakhil FH, Rasheeduzzafar. Effect of Reinforcement Corrosion on Flexural Behavior of Concrete Slabs. J Mater Civ Eng n.d.;8:123–7.

[11] Almusallam A a. Effect of degree of corrosion on the properties of reinforcing steel bars. Constr Build Mater 2001;15:361–8. doi:10.1016/S0950-0618(01)00009-5.

[12] Bairan JM, Marí AR, Ortega H, Rosa JC. Efecto del enrollado y enderezado en las propiedades mecánicas de barras de acero de diámetro medio y grande fabricadas en rollo. Mater Construcción 2011;61:559–81. doi:10.3989/mc.2011.60110.

[13] Garcia MD, Alonso MC, Andrade MC, Rodríguez J. Influencia de la corrosión en las propiedades mecánicas del acero. Hormigón Y Acero 1998;210:11–21.

[14] Moreno Fernández E, Cobo Escamilla A, Fernández Cánovas M. Ductility of reinforcing steel with different degrees of corrosion and the'equivalent steel'criterion. Mater … 2007;57:5–18.

[15] Zhu SLWZXGC. Fatigue of Reinforcing Steel Bars Subjected to Natural Corrosion. Open Civ Eng J 2011:Vol.5, p69. http://connection.ebscohost.com/c/articles/70458995/fatigue-reinforcing-steel-bars-subjected-natural-corrosion (accessed February 14, 2015).

[16] Apostolopoulos C a., Papadopoulos MP. Tensile and low cycle fatigue behavior of corroded reinforcing steel bars S400. Constr Build Mater 2007;21:855–64. doi:10.1016/j.conbuildmat.2005.12.012.

[17] Apostolopoulos CA. Mechanical behavior of corroded reinforcing steel bars S500s tempcore under low cycle fatigue. Constr Build Mater 2007;21:1447–56. doi:10.1016/j.conbuildmat.2006.07.008.

[18] Apostolopoulos A, Matikas T, Apostolopoulos C, Diamantogiannis G. Pit Corrosion Examination of Bare and Embedded Steel Bar. Adv. Met. Mater. Technol., Saint Petersburg: 2013, p. 489–95.

[19] ASTM Standard G1. Standard practice for preparing, cleaning, and evaluating corrosion test specimens 2011.

[20] Maaddawy T El, Soudki K. Effectiveness of impressed current technique to simulate corrosion of steel reinforcement in concrete. J Mater Civ … 2003:41–7.

[21] Badawi M, Soudki K. Control of Corrosion-Induced Damage in Reinforced Concrete Beams Using Carbon Fiber-Reinforced Polymer Laminates. J Compos Constr 2005;9:195–201. doi:10.1061/(ASCE)1090-0268(2005)9:2(195).

[22] Saifullah M, Clark LA. Effect of corrosion rate on the bond strength of corroded reinforcement. In: Press SA, editor. Proc. Int. Conf. Corros. Corros. Prot. steel Concr., University of Sheffield; 1994, p. 591–600.

[23] UNE-EN-ISO-15630-01. Acero para el armado y pretensado del hormigón - Métodos de ensayo. Parte 1: Barras, Alambre y Alambrón para el hormigón armado n.d.

380 [24] Apostolopoulos CA, Demis S, Papadakis VG. Chloride-induced corrosion of steel
381 reinforcement – Mechanical performance and pit depth analysis. Constr Build Mater
382 2013;38:139–46. doi:10.1016/j.conbuildmat.2012.07.087.

383 [25] Misra TU and S. Behavior of Concrete Beams and Columns in Marine Environment When
384 Corrosion of Reinforcing Bars Takes Place 1988:127–46, Vol. 109 SP. doi:10.14359/2796.

385

386

393

394 Table 1. Denomination and standards for grade 500 MPa ductile steel bars

Country	**Standard**	**Denomination for f_y = 500 MPa**
Belgium	NBN A-24-302	BE-5005
France	NF A35-016-1996	FER 500-3
Germany	DIN 488	BST 500 S-IV
Netherlands	NEN 6008	FEB 500 HWL
Spain	UNE 36-065 EX 200	B500S AND B500SD
Switzerland	SIA 262/1 2003	TEMPCORE 500-A
United Kingdom	BS 449:2005	GRADE B500B

395

396 Table 2. Steel characterization of B500SD bars.

Diameter (mm)	**Yielding Load (kN)**	**Ultimate Load (kN)**	**ε_{max}**	**ε_u**	**Modulus of elasticity (GPa)**	**Elastic limit (f_y Mpa)**	**Ultimate stress (f_{max} MPa)**
10	42.62	51.01	0.151	0.189	208	542.56	649.50
12	62.02	72.11	0.13	0.189	197	548.35	637.58

397

398

399

400

401 Table 3. Stress range and applied load to each diameter

Stress Range [MPa]	Diameter [mm]	Max Load [kN]	Min Load [kN]
300	10	23.4	0
	12	33.9	0
200	10	23.4	7.8
	12	33.7	11.3
150	10	-*	-*
	12	25	8.5

*No specimen tested

402

403 Table 4. Specimen list

Specimens	Number
Failed tests	10*
Monotonic test	40
Fatigue tests	142
Total valid specimens	143
Total specimens	192

*Member failed inside the clamps

404

405 Appendix A. Table 1. Monotonic test results

Specimen #	**Corrosion degree (%)**	**Nominal Diameter (mm)**	**Yielding Load (kN)**	**Ultimate Load (kN)**	**ε_{max}**	**ε_u**	**Modulus of Elasticity (GPa)**	**fy* (MPa)**	**fmax* (MPa)**	**Pitting depth (mm) (p)**	**Pitting length (mm) (l)**
MT-10-01	0.0%	10	42.9	51.3	0.152	0.192	208	545.7	652.96	-	-
MT -10-02	0.0%	10	42.4	50.7	0.150	0.185	209	539.5	646.04	-	-
MT -10-03	8.4%	10	34.2	43.4	0.117	0.144	180	474.6	603.52	1.00	6.000
MT -10-04	8.7%	10	33.6	41.2	0.064	0.078	201	468.6	573.66	2.00	5.000
MT -10-05	8.8%	10	32.1	39.7	0.062	0.078	199	448.4	554.73	2.00	9.000
MT -10-06	9.3%	10	33.1	41.4	0.086	0.107	202	464.0	580.85	1.50	13.00
MT -10-07	9.5%	10	32.1	39.4	0.056	0.066	186	451.7	553.31	1.50	9.000
MT -10-08	10 %	10	31.6	39.3	0.059	0.077	204	446.2	555.37	2.50	9.000

MT -10-09	11.1%	10	32.6	40.1	0.069	0.080	206	466.7	574.63	0.50	8.000
MT -10-10	12.6%	10	30.1	38.1	0.061	0.095	205	438.1	554.73	1.00	7.000
MT -10-11	12.9%	10	27.5	34.6	0.041	0.052	185	401.7	504.97	2.00	12.00
MT -10-12	14.3%	10	32.1	40.5	0.101	0.105	163	477.0	600.66	2.00	9.000
MT -10-13	18.5%	10	22.9	29.2	0.037	0.050	132	358.1	456.18	4.00	9.000
MT -12-01	0.0%	12	61.5	72.2	0.126	0.179	206	544.1	638.34	-	-
MT -12-02	0.0%	12	61.4	72.3	0.137	0.191	190	542.5	639.26	-	-
MT -12-03	0.0%	12	63.2	71.8	0.127	0.196	196	558.5	635.14	-	-
MT -12-04	9.1%	12	51.2	62.4	0.076	0.101	201	498.6	607.54	1.00	7.000
MT -12-05	9.6%	12	45.6	57.0	0.107	0.135	153	445.8	557.50	1.50	17.00
MT -12-06	9.7%	12	45.1	55.3	0.080	0.103	150	441.8	541.64	1.50	22.00
MT -12-07	9.7%	12	45.4	55.0	0.071	0.073	175	445.1	538.37	1.00	9.000
MT -12-08	10.7%	12	46.5	57.1	0.090	0.130	161	460.3	565.58	1.00	10.00
MT -12-09	10.8%	12	45.6	56.7	0.069	0.098	173	452.3	561.62	2.00	17.00
MT -12-10	11.1%	12	45.4	58.8	0.090	0.156	134	451.7	585.05	1.50	16.00
MT -12-11	11.3%	12	46.6	57.1	0.079	0.086	161	464.3	569.05	1.00	10.00
MT -12-12	12.0%	12	48.0	57.8	0.086	0.088	158	482.9	580.97	1.50	10.00
MT -12-13	12.1%	12	44.7	54.0	0.070	0.100	161	449.5	542.82	2.50	14.00
MT -12-14	12.2%	12	44.8	53.7	0.066	0.085	166	451.0	541.13	1.50	7.000
MT -12-15	12.4%	12	43.0	54.2	0.071	0.094	138	433.8	546.83	2.50	26.00
MT -12-16	14.6%	12	44.9	55.9	0.073	0.100	186	464.5	578.72	0.50	7.000
MT -12-17	14.9%	12	45.1	55.5	0.070	0.105	196	468.4	576.68	2.00	24.00
MT -12-18	15.0%	12	40.4	51.4	0.063	0.087	170	420.4	534.09	1.80	21.00
MT -12-19	16.8%	12	36.9	47.6	0.054	0.073	145	392.0	506.21	2.00	12.00
MT -12-20	16.9%	12	39.2	48.7	0.062	0.081	151	416.9	518.88	2.00	12.00
MT -12-21	17.5%	12	38.1	44.9	0.032	0.040	161	408.3	481.01	3.00	21.00
MT -12-22	17.9%	12	40.1	50.1	0.074	0.114	158	431.6	539.70	1.50	6.000
MT -12-23	19.6%	12	38.2	44.8	0.037	0.037	157	420.3	492.62	2.50	11.00
MT -12-24	19.7%	12	34.5	42.0	0.040	0.059	147	379.3	462.02	3.50	8.000
MT -12-25	19.78%	12	36.5	44.2	0.058	0.076	131	402.2	487.23	3.00	73.00
MT -12-26	21.4%	12	34.9	42.3	0.037	0.059	223	392.7	475.93	3.00	18.00
MT -12-27	21.5%	12	35.0	39.2	0.027	0.036	165	394.0	442.14	3.00	17.00

406

407 Appendix A. Table 2. Fatigue test results and pitting characterization

Specimen #	**Corrosion degree (%)**	**Nominal diameter (mm)**	**Pitting description**		**Stress range (MPa)***	**Resisted cycles (N)**
			Depth (mm) (p)	**Length (mm) (l)**		
	10					
FT-10-01		10	1.50	17.00	200	102,030
FT-10-01	9.2%	10	1.00	12.00	300	99,027
FT-10-02	10.7%	10	1.00	6.000	300	82,951

FT-10-03	10.8%	10	2.00	14.00	200	192,984
FT-10-04	11.1%	10	2.00	10.00	200	74,703
FT-10-05	11.3%	10	1.00	21.00	300	122,934
FT-10-06	12.3%	10	1.00	14.00	300	55,970
FT-10-07	12.4%	10	1.00	4.000	300	44,883
FT-10-08	12.5%	10	1.00	5.000	200	254,568
FT-10-09	15.1%	10	2.00	8.000	200	167,236
FT-10-10	15.7%	10	0.50	6.000	300	64,691
FT-10-11	17.2%	10	2.50	14.00	200	31,959
FT-10-12	17.2%	10	2.00	16.00	300	5,715
FT-10-13	17.7%	10	1.50	27.00	200	146,670
FT-10-14	17.9%	10	1.50	22.00	300	8,603
FT-10-15	20.3%	10	2.50	21.00	200	5,706
FT-10-16	20.3%	10	2.00	37.00	200	55,508
FT-10-17	20.5%	10	2.50	19.00	300	3,157
FT-10-18	20.6%	10	3.00	11.00	300	99
FT-10-19	21.8%	10	1.00	8.000	300	12,959
FT-10-20	21.8%	10	2.50	15.00	200	16,346
FT-10-21	22.8%	10	2.00	53.00	200	35,988
FT-10-22	23.2%	10	2.00	82.00	200	68,742
FT-10-23	25.1%	10	2.50	47.00	300	2,649
FT-10-24	25.2%	10	2.50	23.00	300	1,785
FT-12-01	8.6%	12	1.50	77.00	200	266,070
FT-12-02	8.7%	12	1.50	9.000	300	134,401
FT-12-03	8.7%	12	1.50	17.00	150	943,043
FT-12-04	9.7%	12	1.00	8.000	200	325,922
FT-12-05	10.3%	12	1.50	27.00	300	94,433
FT-12-06	10.4%	12	1.50	23.00	200	325,956
FT-12-07	10.8%	12	1.50	6.000	200	438,070
FT-12-08	10.8%	12	2.00	36.00	200	267,542
FT-12-09	10.9%	12	2.00	36.00	200	153,870
FT-12-10	10.9%	12	1.50	44.00	300	64,620
FT-12-11	11.2%	12	2.00	13.00	200	264,010
FT-12-12	11.2%	12	2.00	60.00	150	372,276
FT-12-13	11.5%	12	1.50	24.00	200	374,083
FT-12-14	11.6%	12	2.00	27.00	200	245,160
FT-12-15	11.6%	12	1.50	12.00	300	91,536
FT-12-16	11.6%	12	1.50	70.00	300	87,416
FT-12-17	11.7%	12	1.50	14.00	200	256,383
FT-12-18	11.7%	12	1.00	10.00	300	108,497
FT-12-19	12.2%	12	2.00	8.000	300	28,050
FT-12-20	12.2%	12	2.00	11.00	150	583,245
FT-12-21	12.6%	12	2.00	15.00	200	126,155
FT-12-22	12.7%	12	1.00	4.000	300	60,355
FT-12-23	13.0%	12	2.00	15.00	200	343,394

FT-12-24	13.1%	12	2.00	10.00	300	29,815
FT-12-25	13.2%	12	2.00	31.00	300	56,650
FT-12-26	13.3%	12	2.00	27.00	200	132,471
FT-12-27	13.4%	12	1.50	13.00	300	62,138
FT-12-28	13.4%	12	2.00	14.00	200	90,750
FT-12-29	13.6%	12	2.00	43.00	200	129,033
FT-12-30	13.6%	12	1.50	13.00	300	63,818
FT-12-31	13.7%	12	2.00	52.00	300	18,182
FT-12-32	13.7%	12	2.00	16.00	200	395,720
FT-12-33	13.7%	12	2.00	6.000	200	112,996
FT-12-34	14.1%	12	2.00	15.00	200	40,007
FT-12-35	14.1%	12	1.00	13.00	300	51,259
FT-12-36	14.2%	12	1.50	14.00	300	24,711
FT-12-37	14.3%	12	1.50	7.000	200	151,373
FT-12-38	14.3%	12	3.00	19.00	300	11,548
FT-12-39	14.4%	12	1.00	7.000	200	283,849
FT-12-40	14.4%	12	1.50	10.00	300	42,910
FT-12-41	14.5%	12	2.00	11.00	200	132,905
FT-12-42	14.5%	12	2.00	14.00	200	179,672
FT-12-43	14.5%	12	1.00	8.000	300	64,468
FT-12-44	14.5%	12	2.00	21.00	300	11,751
FT-12-45	14.5%	12	2.00	12.00	200	160,378
FT-12-46	14.6%	12	2.00	29.00	200	99,873
FT-12-47	14.8%	12	1.50	12.00	200	149,582
FT-12-48	14.9%	12	2.00	12.00	200	155,094
FT-12-49	14.9%	12	2.00	11.00	200	99,365
FT-12-50	15.0%	12	1.50	54.00	300	68,504
FT-12-51	15.0%	12	2.50	16.00	200	39,134
FT-12-52	15.2%	12	1.50	33.00	300	92,051
FT-12-53	15.2%	12	2.50	21.00	200	111,312
FT-12-54	15.6%	12	2.00	12.00	200	178,298
FT-12-55	15.8%	12	1.50	8.000	300	48,224
FT-12-56	16.1%	12	2.00	12.00	150	556,891
FT-12-57	16.1%	12	2.00	12.00	200	266,610
FT-12-58	16.1%	12	2.00	12.00	300	12,100
FT-12-59	16.2%	12	2.00	19.00	150	574,851
FT-12-60	16.3%	12	3.00	29.00	200	23,509
FT-12-61	16.6%	12	2.00	22.00	200	54,991
FT-12-62	16.6%	12	1.50	13.00	300	42,581
FT-12-63	16.8%	12	2.50	49.00	300	13,192
FT-12-64	17.1%	12	2.00	12.00	200	81,724
FT-12-65	17.2%	12	2.50	31.00	200	48,511
FT-12-66	17.2%	12	2.50	72.00	300	42,505
FT-12-67	17.3%	12	2.50	58.00	200	78,338
FT-12-68	17.3%	12	2.00	20.00	300	27,798

FT-12-69	17.3%	12	2.00	32.00	200	146,772
FT-12-70	17.3%	12	1.50	11.00	200	109,014
FT-12-71	17.5%	12	3.00	44.00	200	73,150
FT-12-72	17.5%	12	1.50	11.00	300	40,084
FT-12-73	17.5%	12	2.00	51.00	200	49,011
FT-12-74	17.5%	12	2.00	32.00	300	54,870
FT-12-75	17.6%	12	2.00	16.00	300	13,494
FT-12-76	17.7%	12	3.00	23.00	150	324,138
FT-12-77	17.7%	12	2.00	19.00	300	22,164
FT-12-78	17.8%	12	3.00	31.00	300	3,095
FT-12-79	17.9%	12	2.50	31.00	300	11,582
FT-12-80	17.9%	12	3.00	20.00	200	95,451
FT-12-81	17.9%	12	2.50	28.00	150	119,620
FT-12-82	17.9%	12	2.00	7.000	200	32,852
FT-12-83	17.9%	12	1.00	30.00	300	147,678
FT-12-84	18.2%	12	2.00	12.00	200	159,922
FT-12-85	18.3%	12	2.00	12.00	300	12,353
FT-12-86	18.3%	12	3.00	34.00	300	7,405
FT-12-87	18.4%	12	1.50	17.00	200	79,579
FT-12-88	18.6%	12	1.50	52.00	300	43,900
FT-12-89	18.9%	12	2.50	18.00	200	117,108
FT-12-90	19.0%	12	4.00	39.00	150	14,767
FT-12-91	19.1%	12	2.50	53.00	200	18,025
FT-12-92	19.3%	12	2.00	23.00	300	10,613
FT-12-93	19.3%	12	3.50	27.00	200	2,780
FT-12-94	19.5%	12	3.00	27.00	200	37,538
FT-12-95	19.6%	12	2.00	23.00	300	18,255
FT-12-96	19.6%	12	3.00	24.00	200	13,850
FT-12-97	20.1%	12	2.50	24.00	150	200,597
FT-12-98	20.3%	12	3.00	31.00	300	898
FT-12-99	20.6%	12	3.00	57.00	200	5,909
FT-12-100	21.0%	12	3.00	40.00	300	10,490
FT-12-101	21.1%	12	2.00	29.00	300	10,010
FT-12-102	21.2%	12	2.50	23.00	200	51,428
FT-12-103	21.4%	12	2.50	27.00	200	63,863
FT-12-104	21.5%	12	3.00	62.00	200	7,485
FT-12-105	21.7%	12	2.50	27.00	300	3,453
FT-12-106	22.5%	12	4.00	13.00	200	156
FT-12-107	23.2%	12	3.00	66.00	200	25,064
FT-12-108	23.8%	12	4.00	24.00	150	11,208
FT-12-109	23.9%	12	3.00	82.00	150	26,411
FT-12-110	24.1%	12	3.00	39.00	200	887
FT-12-111	25.3%	12	2.00	21.00	300	3,200
FT-12-112	27.6%	12	4.00	41.00	150	6,459

*Stress range considering the nominal diameter

408
409

410

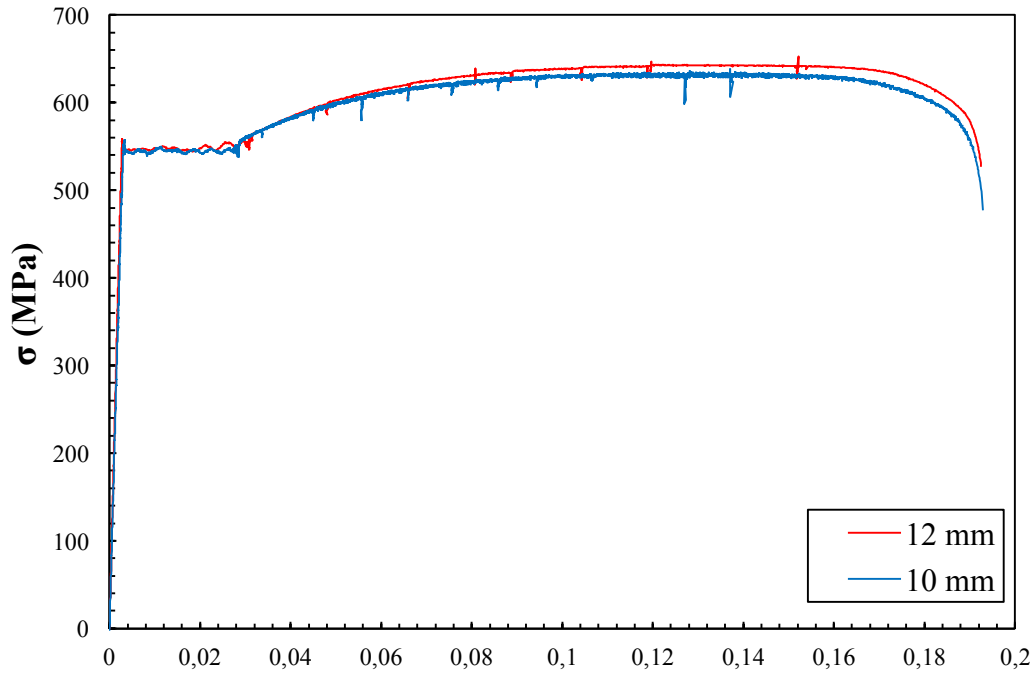

Figure 1. Stress-strain behaviour of uncorroded B500SD bars.

Figure 2. Statically indeterminate corroded beams and extracted steel reinforcement

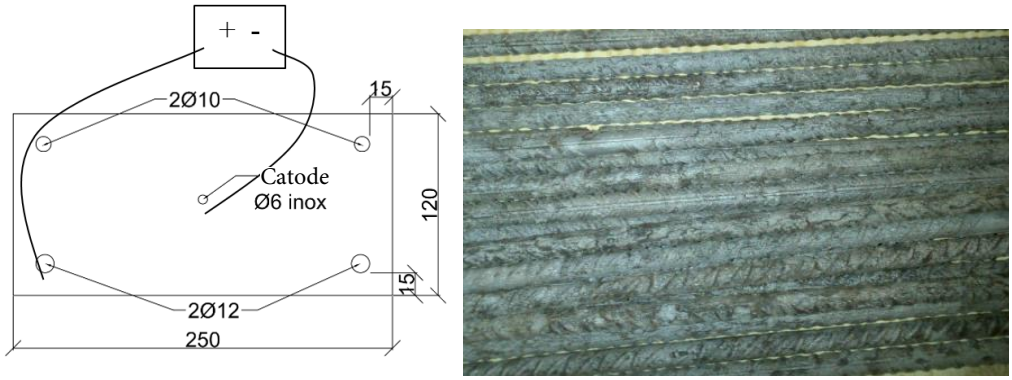

Figure 3. a) Induced corrosion scheme, b) Cleaned bars by means of sand cleaner

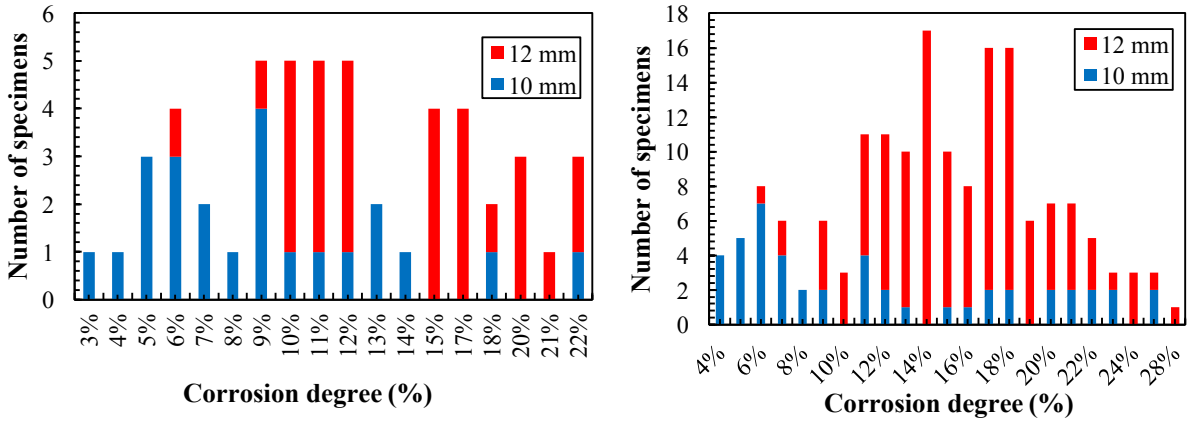

Figure 4. Test member distribution with respect to the corrosion degree, a) monotonic test b) fatigue test

Figure 5. Test setup description monotonic and fatigue

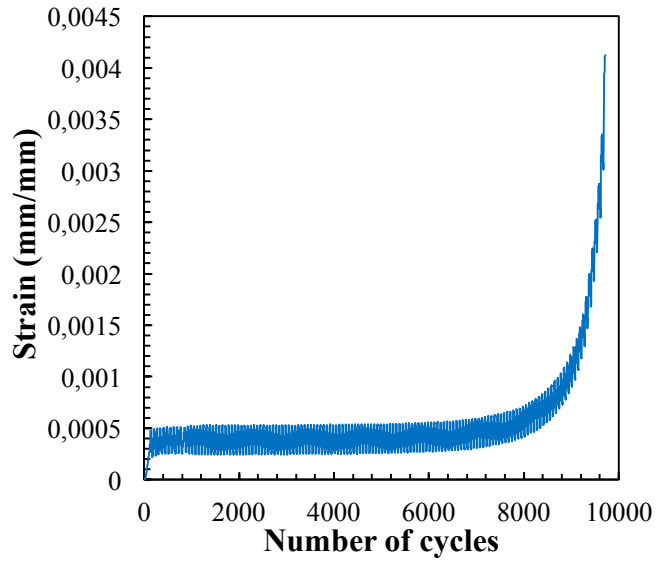

Figure 6. Strain recorded vs N cycles by means of the disposed transducer. Accumulative damage on the bar

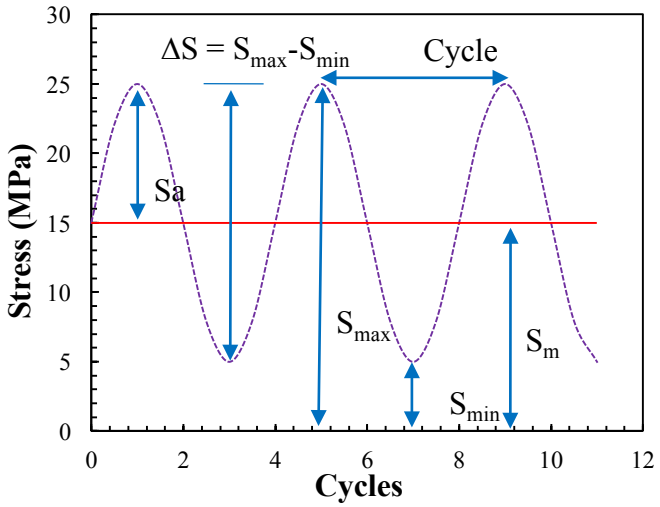

Figure 7. Sinusoidal loading curve for fatigue test

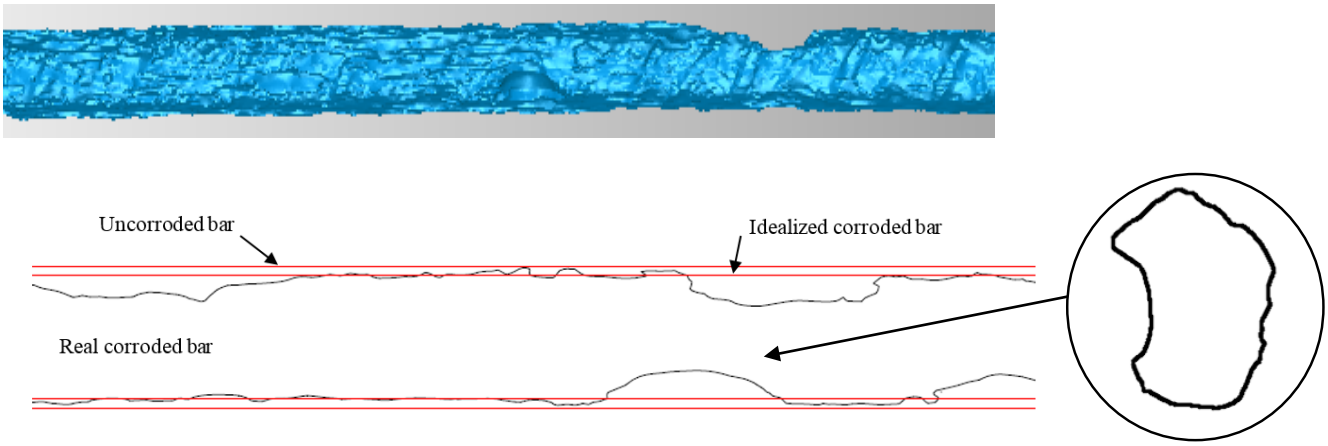

Figure 8. a) Pit distribution. Idealized and nominal cross-section b) Real critical cross-section

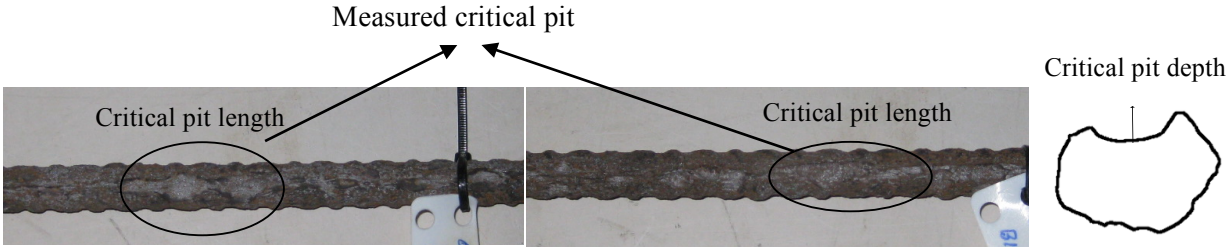

Figure 9. Pit definition in the critical cross-section

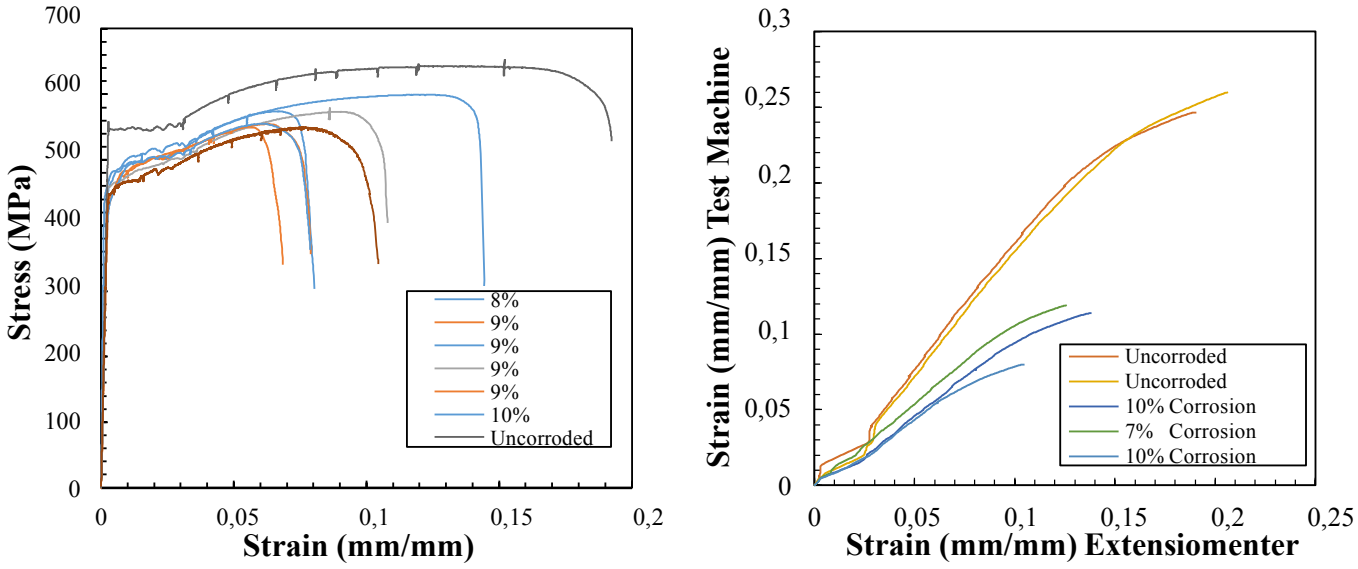

Figure 10. a) σ-ε curve corroded specimens 8%-10% corrosion degree b) ε test machine vs ε extensometer

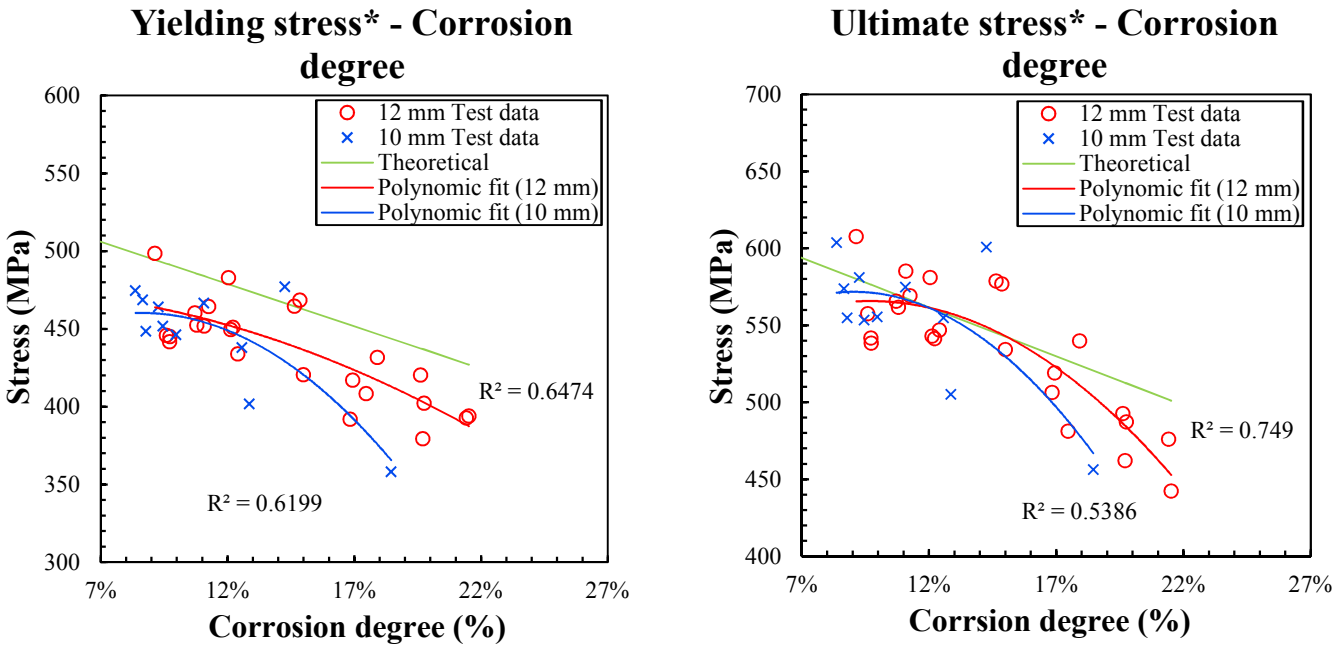

Figure 11. Elastic limit load and ultimate load vs. corrosion degree

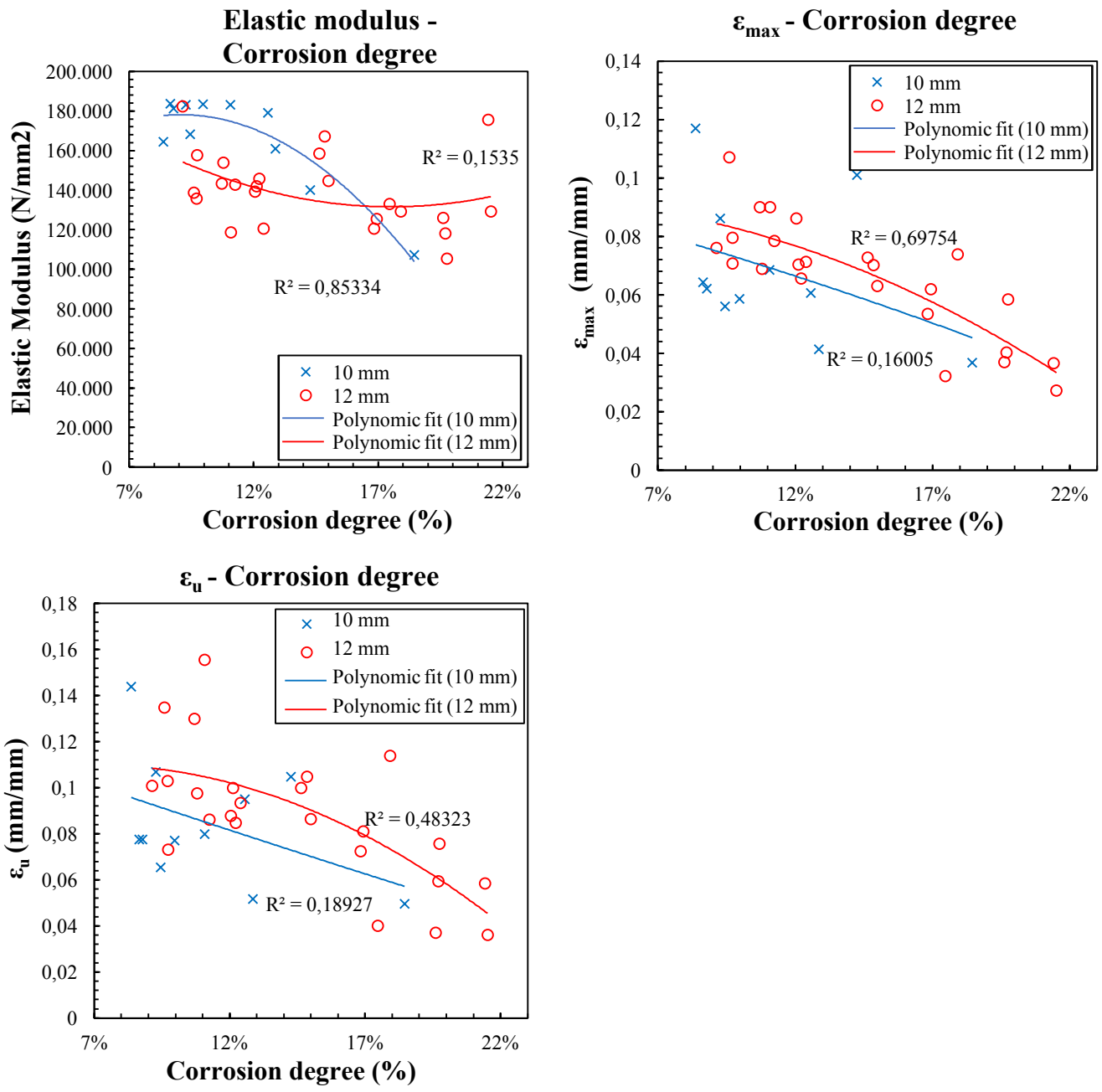

Figure 12. Elastic modulus, maximum ε and ultimate ε with respect to the corrosion degree.

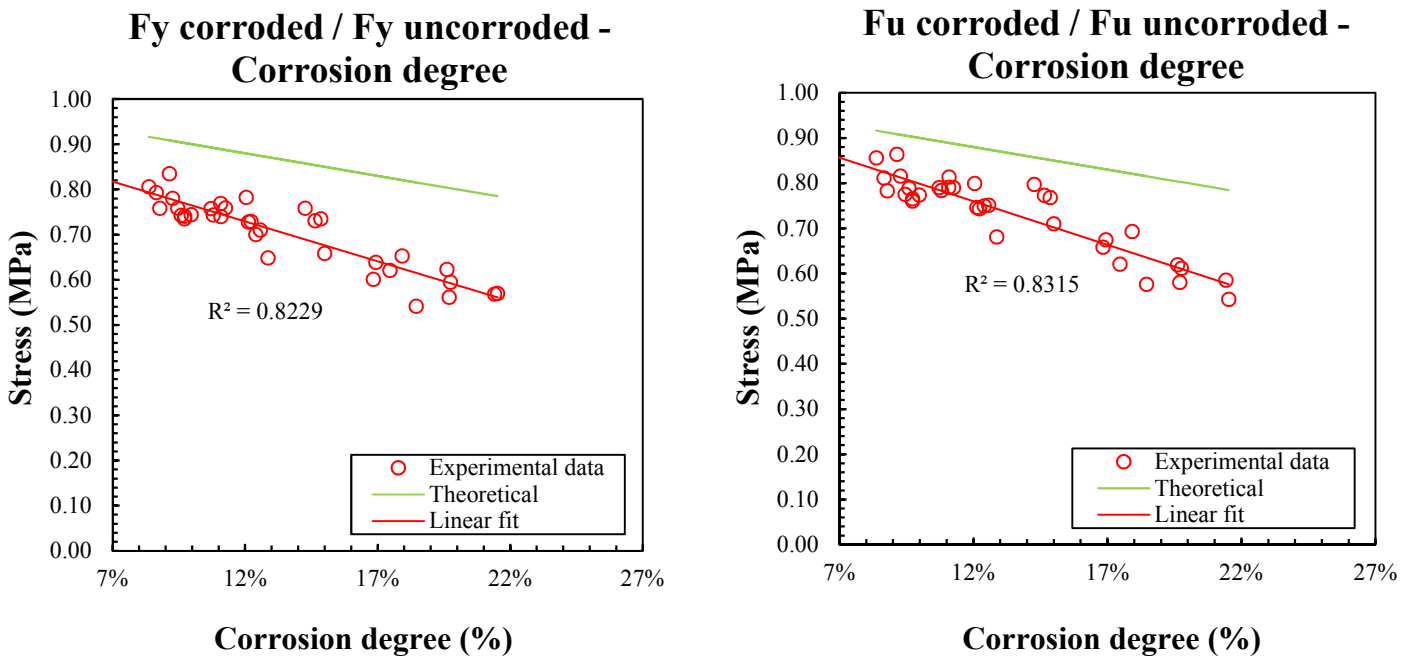

Figure 13. Reduction of ultimate stress and yielding stress ratios with respect to those of uncorroded steel and corrosion degree for 12 mm and 10 mm diameter

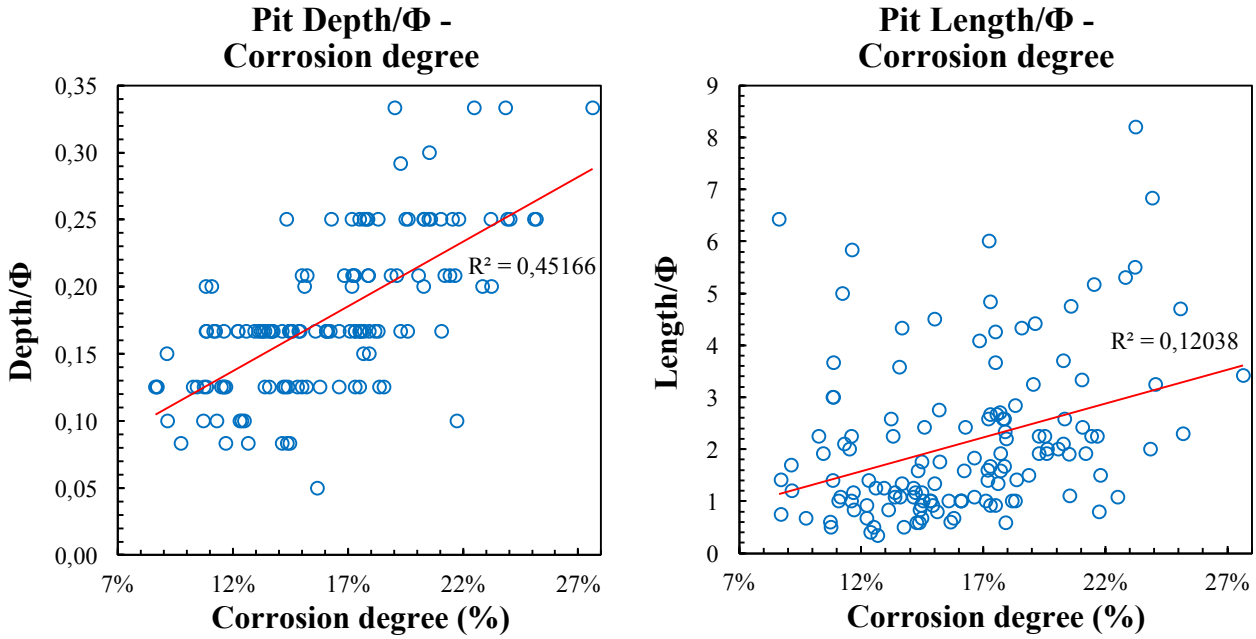

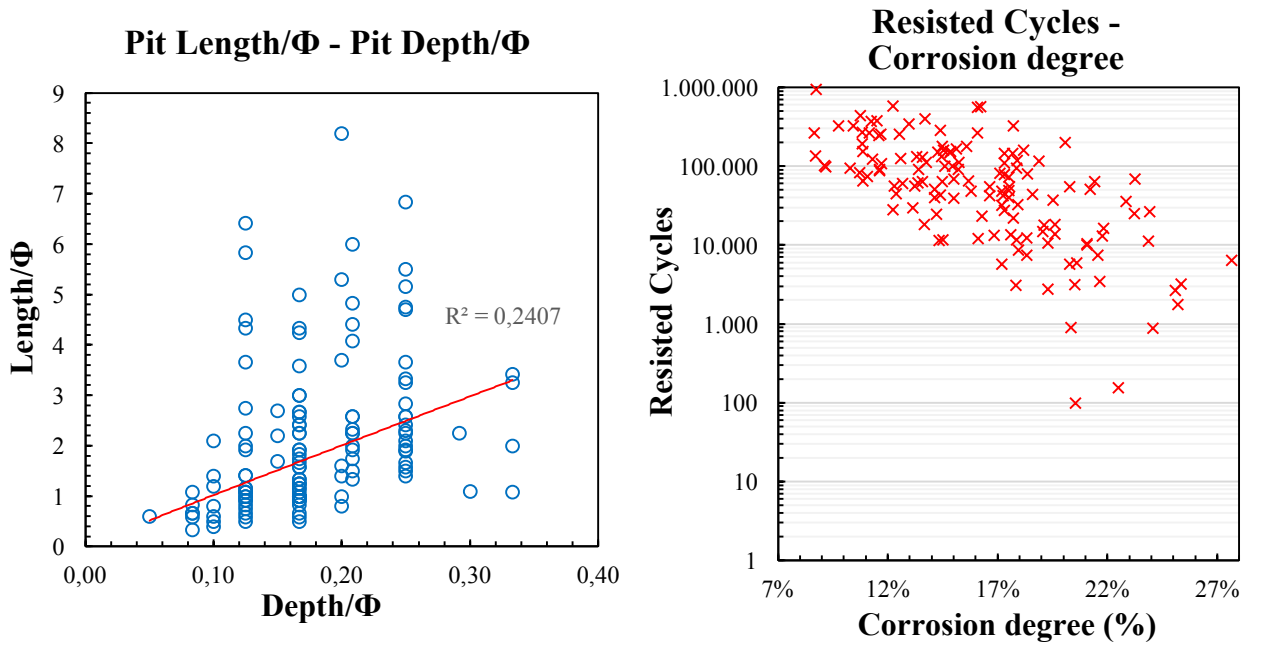

Figure 14. Pit characteritzation with respect to corrosion degree and fatigue life results

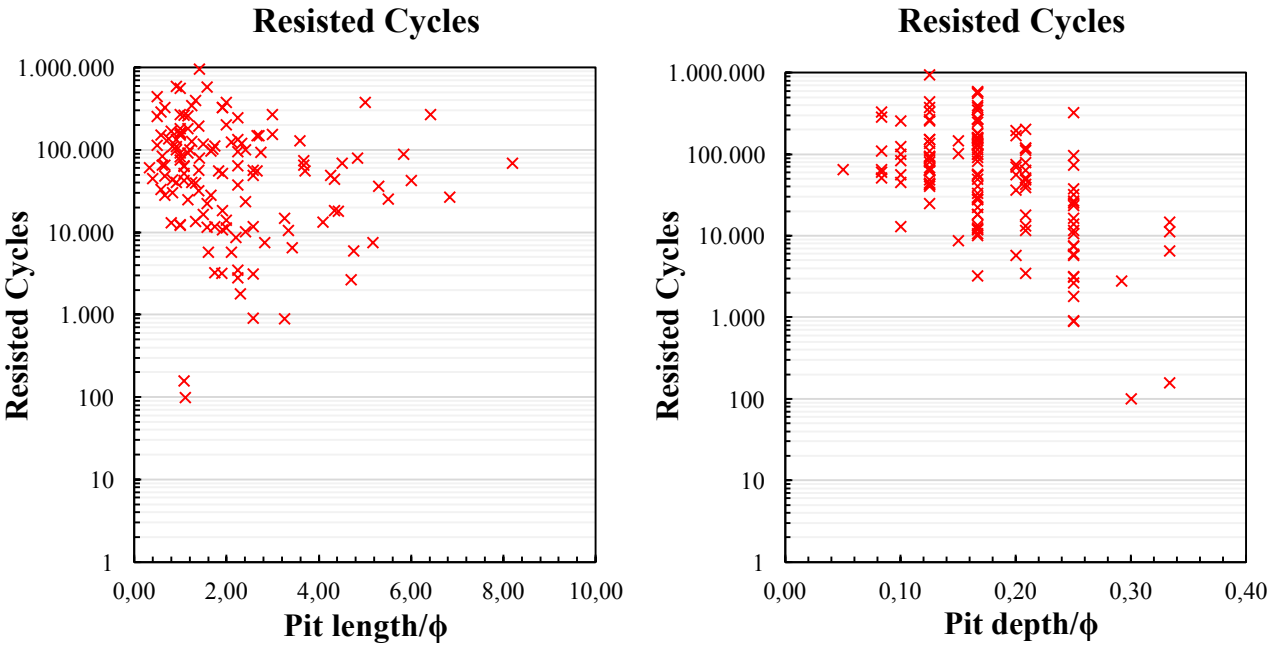

Figure 15. Registered fatigue life with respect to the pit parameters

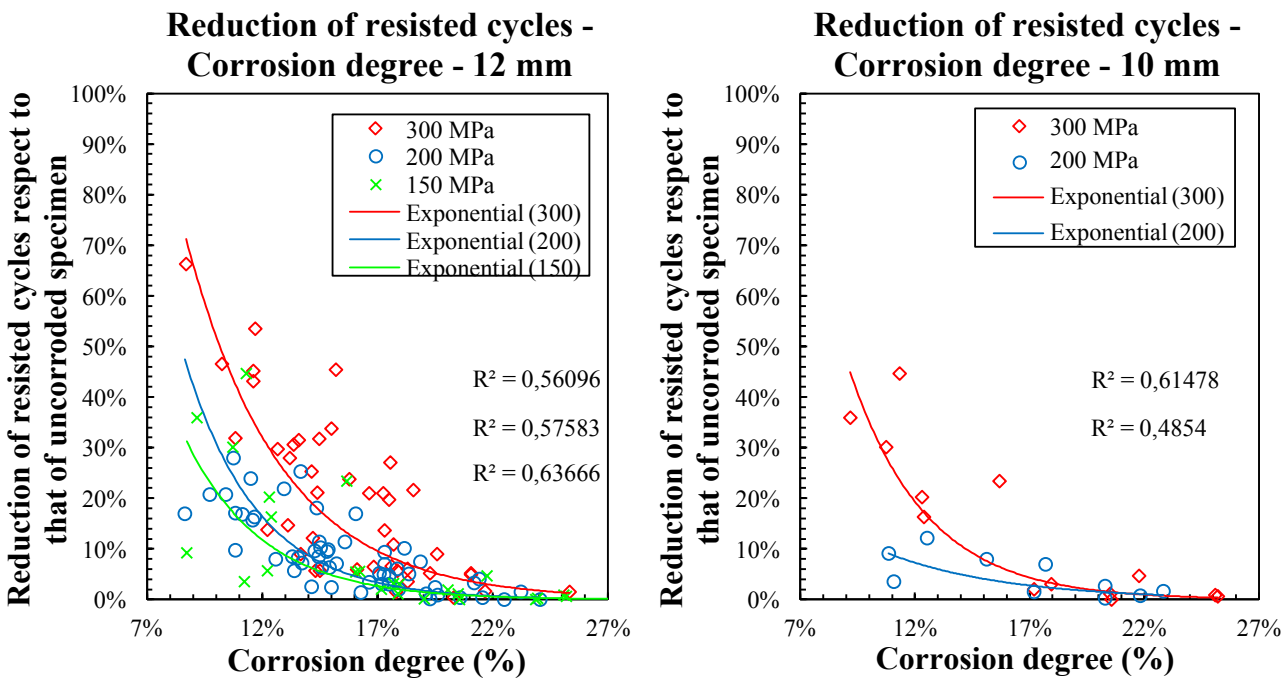

Figure 16. Fatigue life of corroded specimens. 12 mm and 10 mm diameter bars